Supporting Information

Multi-Functional Integrated Design of High-Performance Cathode for Lithium-Oxygen Batteries

Jing Lan, Yuran Yu, Fujun Miao*, Peng Zhang* and Guosheng Shao*

State Center for International Cooperation on Designer Low-Carbon and Environmental Materials (CDLCEM), School of Materials Science and Engineering, Zhengzhou University, 100 Kexue Avenue, Zhengzhou 450001, China

Zhengzhou Materials Genome Institute (ZMGI), Zhongyuanzhigu, Xingyang, Zhengzhou 450100, China

*Corresponding author: miaofj@zzu.edu.cn; zhangp@zzu.edu.cn; gsshao@zzu.edu.cn

Synthesis and Preparation

Chemicals and Materials : Cu Foam was obtained from Tianjin Yingke Haozhi Technology Co. Ltd.Ammonium persulfate $((NH_4)_2S_2O_8)$, Sodium hydroxide (NaOH), Ethyl alcohol (C_2H_6O), $NH_3 \cdot H_2O$ were purchased from Sinopharm Chemical Reagent Co. Ltd. Sodium citrate(99%), Gold chloride trihydrate($HAuCl_4 \cdot 3H_2O$), tetraethylene glycol dimethyl ether (TEGDME), and lithium bis(trifluoromethanesulphonyl)imide (LiTFSI), Lithium nitrate $(LiNO_3, 99.99\%)$ and Lithium iodide (LiI, 99.9%), were purchased from Aladdin Reagent.

Synthesis of CuFo-Cu(OH)$_2$ nanowires : Cu foam (CuFo) was cleaned with hydrochloric acid, and ethanol, distilled water three times, and vacuumized. The cleaned CuFo (tailored into circle shape with a diameter of 12mm) was then immersed into a mixed solution of $(NH_4)_2S_2O_8$ (0.75 M) and NaOH (1.875 M) for 20 min at room temperature, ensuring $Cu(OH)_2$ grown on CuFo (CuFo-Cu(OH)$_2$ nanowires). The sample was taken out from the solution, washed with distilled water three times, dried at 60 °C in air.

Preparation of CuFo-Cu@C Nanowires : The as prepare CuFo-Cu(OH)$_2$ Nanowires was soaked in a mixture of 20 mL ethanol, 4 ml distilled water, 1.5 mL ammonia solution, 0.225 mL formaldehyde solution and 0.15 g resorcinol overnight. By annealing the above obtained CuFo-

Cu(OH)$_2$@resorcinol formaldehyde (RF) nanowires in a tube furnace at 500°C for 0.5 h under Ar atmosphere and continue to heat up to 700°C for 0.5 h at a heating rate of 2°C min^{-1} under the 8% Ar/H$_2$ atmosphere, the CuFo-Cu@C Nanowires was fabricated. Moreover, the direct reduction of as-prepared CuFo-Cu(OH)$_2$ nanowires was at 400 °C for 0.5 h under 8% Ar/H$_2$ atmosphere, denoting as CuFo-Cu. It should be noted that the Cu-based nanowires would be disappeared if without the protection of function coating layer.

Preparation of CuFo-Cu@C/Au nanowires and CuFo-Cu/Au : To prepare gold nanoparticles on CuFo-Cu@C nanowires, a classic recipe was used. Typically, 1 ml sodium citrate was diluted in 100 ml water. After the solution to boiling, 200 ul chloroauric acid (HAuCl$_4$, 0.5 M) and the CuFo-Cu@C NWs were quickly injected. The reaction was allowed for 10 min and the sample was taken out from the solution to obtain the CuFo-Cu@C/Au NWs. The CuFo-Cu/Au could be obtained by the same method.

Characterization: The morphologies and detailed structures of samples were investigated by Scanning Electronic Microscopy (SEM, ZEISS SIGMA 500, operating at 5 kV attached with a Bruker energy dispersive X-ray spectrometer); Transmission Electron Microscope (TEM), Scanning Transmission Electron Microscopy (STEM), X-ray Photoelectron Spectroscopy (XPS) was carried out on AXIS Supra and all data were calibrated with the C 1s of 284.8 eV , Energy Dispersive X-ray

spectroscopy (EDX) and Selected Area Electron Diffraction (SAED) were operated at 200 kV with a cold field emission source (FEI Tecnai G2 F20). Raman spectrum was on Horiba LabRAM HR Evolution Spectrometer with a 532 nm excitation wavelength; X-ray Diffraction (XRD) was conducted using a Rigaku Ultima IV system with Cu Kα radiation. Nitrogen adsorption/desorption isotherm was analyzed on an ASAP 2020.

Li-O$_2$ battery assemble and test: The assemble processes of 2032-type coin cells were conducted in an Ar-filled glove box, in which the lithium foil, the obtained CuFo-Cu@C/Au NWs (with a diameter of 12 mm), and a glass fiber serves as anode, cathode and separator, respectively. The applied electrolyte of TEGDME with containing 1 M LiTFSI with 0.2 M LiNO$_3$ and 0.2 M LiI with a dosage of 100 μL. The electrochemical performances of the cathodes were examined at a limited capacity with different current densities. The charge-discharge curve and cycle performance was performed by a Land CT2001A battery analyzer. The EIS study was conducted by the CHI660 electrochemical station with a frequency between 10 mHz and 100 kHz. The cyclic voltammetry (CV) curves were carried out between 2.0 and 4.5 V with a scan rate of 1 mV s^{-1}

Computational simulation: Theoretical calculations were performed in the framework of the density functional theory (DFT), using the Vienna Ab Initio Simulation Package (VASP),[1,2] with the projector augmented wave

(PAW) method with a cutoff energy of 500 eV for the ionic potentials including the overall effect of core electrons. [3,4] For the geometric relaxation of the structures, summation over the Brillouin Zone (BZ) is performed with $3 \times 3 \times 2$ Monkhorst-Pack k-point meshes for the Au-C plane (82 atoms). Slab model for Au-C layer was constructed with a vacuum layer of 15 Å in the z direction to avoid the interaction between layers. Optimized structures were obtained by minimizing the forces on each ion until they fell below 0.05 eV/Å.[5] The Density of States needs to be calculated to elucidate the catalytic performance of different materials using the hybrid functionals HSE06.[6-9] All calculations were spin-polarized.

the Gibbs free energy of each reaction step can be expressed as:

$$\Delta G_1 = \left(G_{LiO_2\,*} + 3G_{Li}\right) - \left(G_* + G_{O_2} + 4G_{Li}\right)$$

(1)

$$\Delta G_2 = \left(G_{Li_2O_2\,*} + 2G_{Li}\right) - \left(G_{LiO_2\,*} + 3G_{Li}\right)$$

(2)

$$\Delta G_3 = \left(G_{(Li_2O_2)_2\,*}\right) - \left(G_{Li_2O_2\,*} + G_{O_2} + 2G_{Li}\right)$$

(3)

where G_*, $G_{LiO_2\,*}$, $G_{Li_2O_2\,*}$ and $G_{(Li_2O_2)_2\,*}$ represent the energies of the catalyst surface and the catalyst surface with LiO_2, Li_2O_2 and $(Li_2O_2)_2$ adsorbates. G_{Li} and G_{O_2} are the energy of a single Li atom and an isolated gas molecule O_2. For each adsorption configuration, the Gibbs free energy should be corrected for the adsorption groups will vibrate at different orientations. The corrected value, ΔE is obtained through VASPKIT software by the following equation: [5]

$$\Delta E = ZPE - TS \qquad (4)$$

where ZPE, T and S are the zero-point energy, temperature, and entropy.

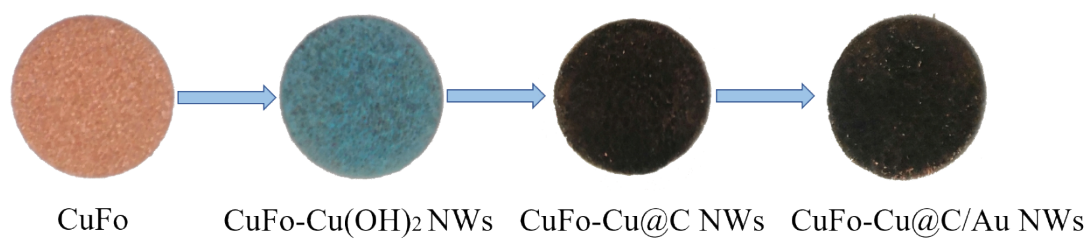| CuFo | CuFo-Cu(OH)$_2$ NWs | CuFo-Cu@C NWs | CuFo-Cu@C/Au NWs |

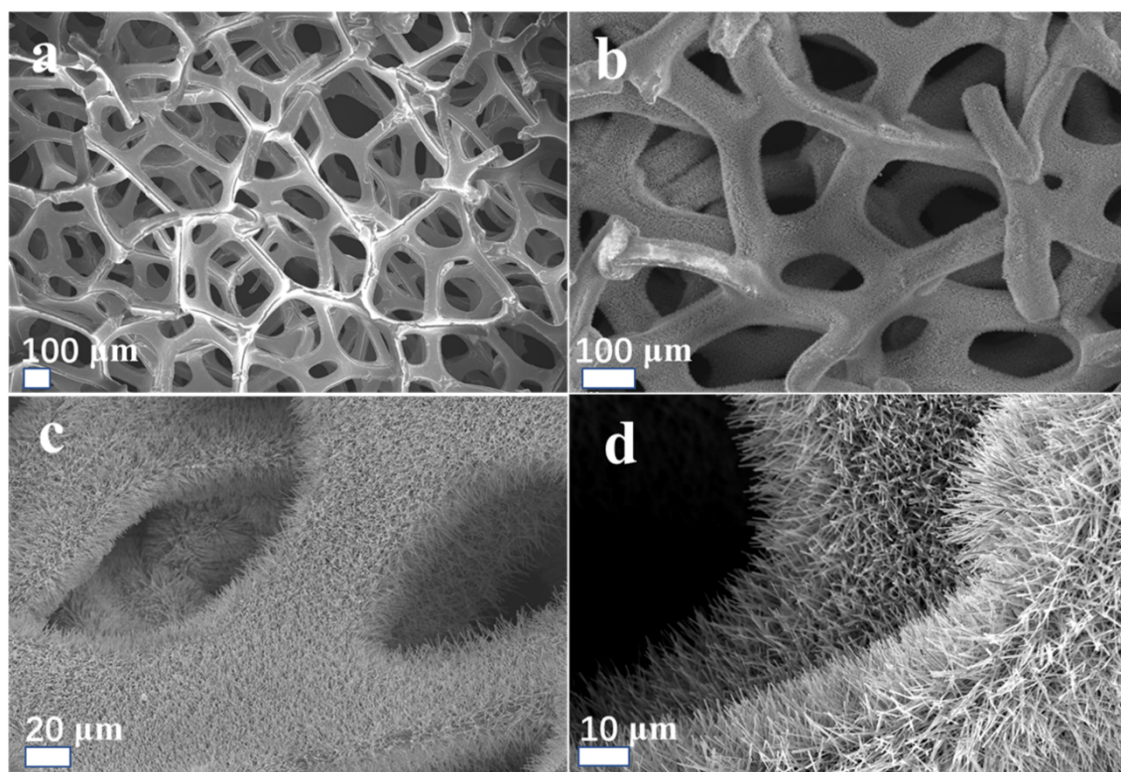**Figure S1**. Optical photograph for the fabrication process of CuFo-Cu@C/Au NWs.

Figure S2. (a) SEM image of pure Cu foam. (b), (c) and (d) SEM images of CuFo supported $Cu(OH)_2$ nanowires, respectively. Obviously, a dense and uniform $Cu(OH)_2$ nanowires are grown on the surface of CuFo.
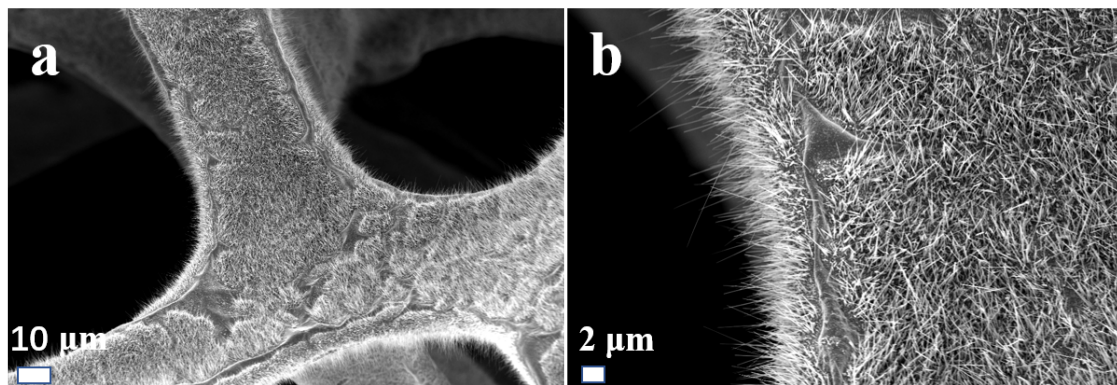
Figure S3. SEM images of the CuFo-CuO nanowires fabricated by thermal oxidation method. It should be noted that is very difficult to achieve dense and large-area uniform Cu-based nanowires on CuFo.
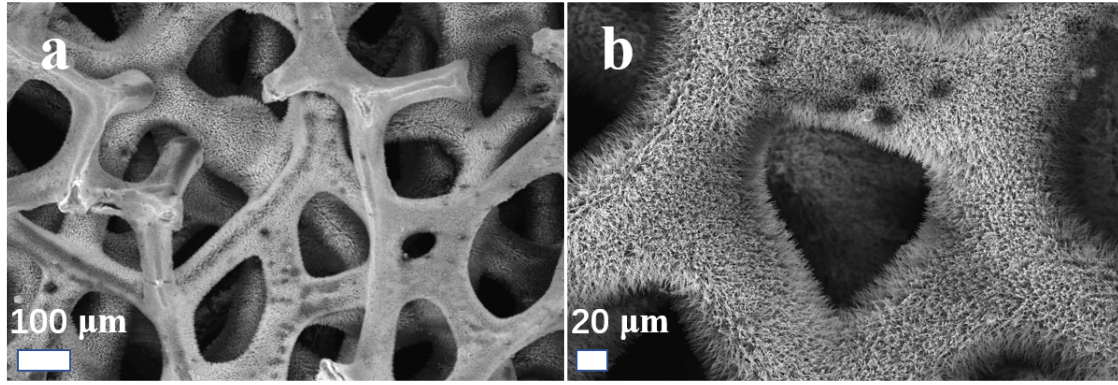
Figure S4. SEM images of CuFo-Cu(OH)$_2$@RF nanowires.
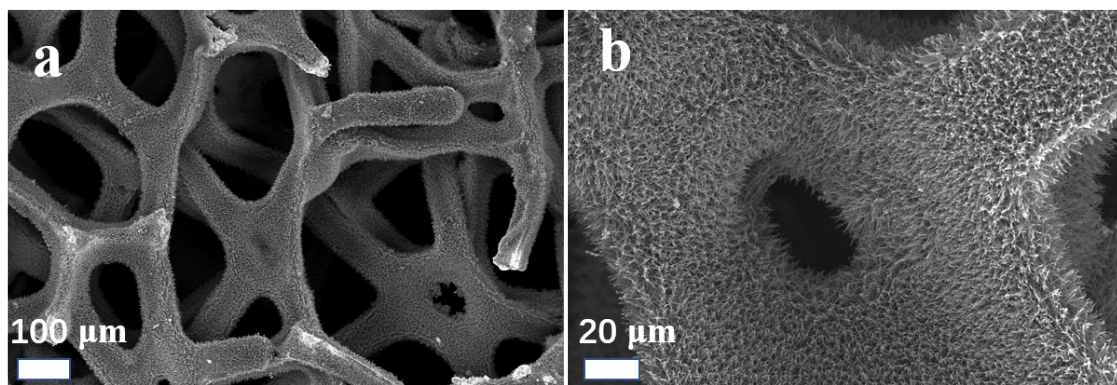
Figure S5. SEM images of CuFo-Cu@C nanowires under different magnifications. It can be clearly observed that the dense and uniform Cu@C core-shell nanowire supported on CuFo are well preserved without destruction after the reduction process due to the well-designed functional protecting layer.
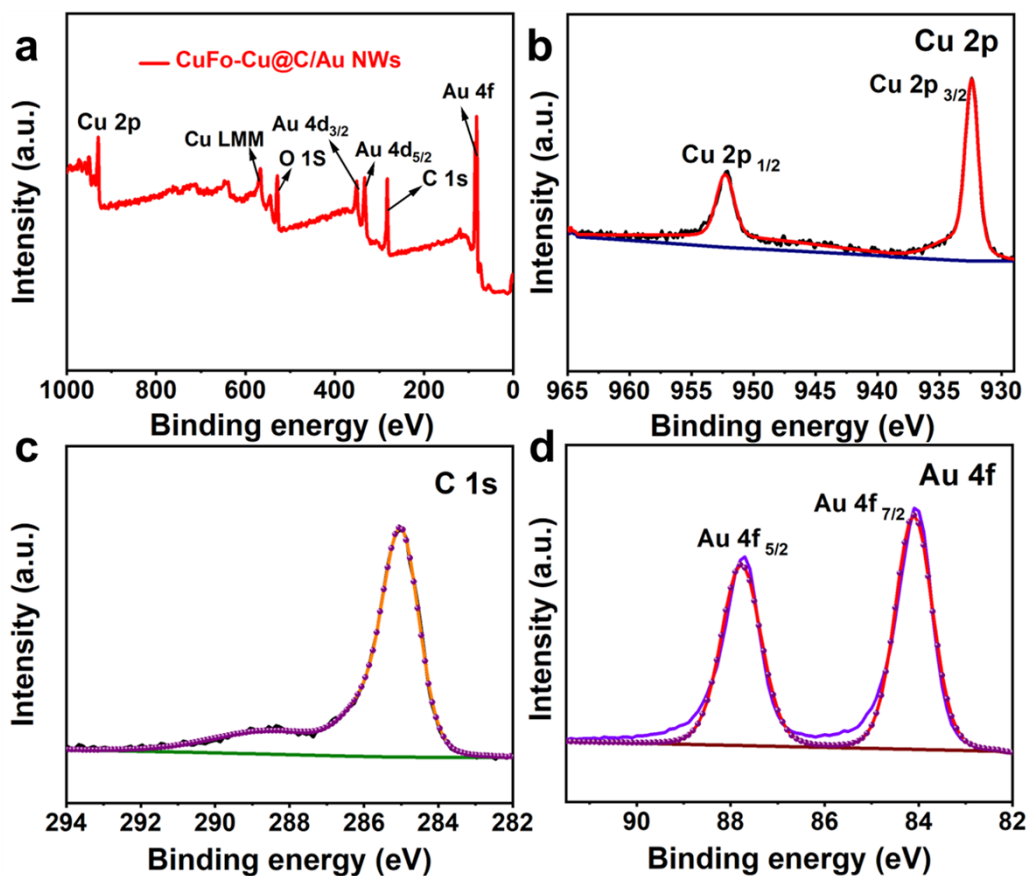
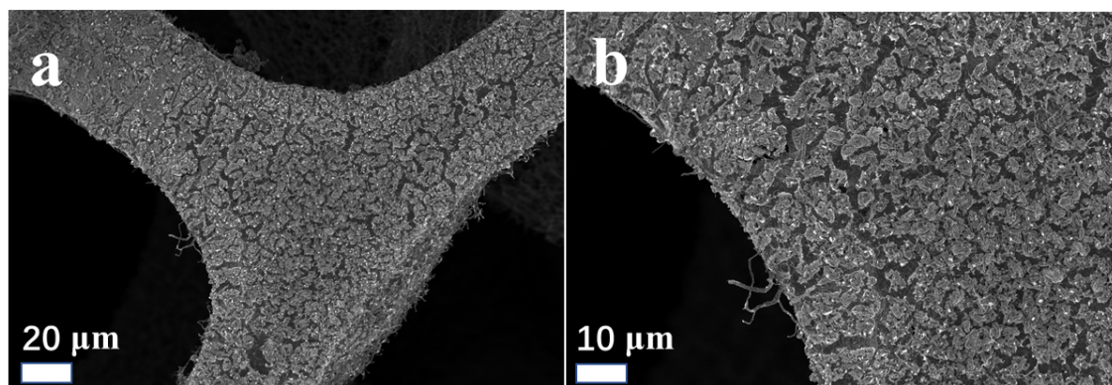**Figure S6**. (a) XPS survey spectra of CuFo-Cu@C/Au NWs, (b) to (d) high-resolution XPS spectra of Cu 2p, C 1s and Au 4f, respectively.

Figure S7. SEM images of the CuFo-Cu. The CuFo-Cu(OH)$_2$ nanowires without the functional protecting layer will result in the collapse of nanowire after the annealing reduction process, further demonstrating the importance of the protecting layer in the well-designed hierarchical structure.
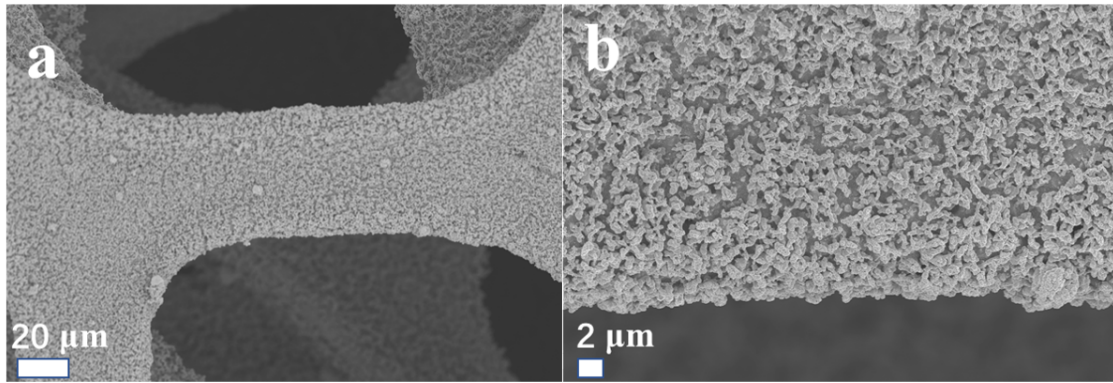
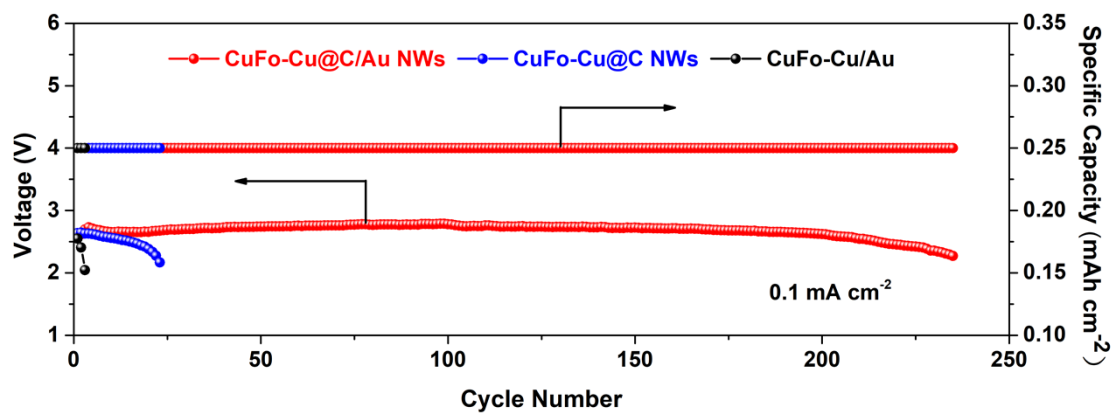**Figure S8.** SEM images of the CuFo-Cu/Au as comparison sample.

Figure S9. Discharge voltage versus cycle number for the cathodes of CuFo-Cu@C/Au NWs, CuFo-Cu@C NWs and CuFo-Cu/Au with 0.1 mA cm^{-1} at a fixed capacity of 0.25 mAh cm^{-1}.
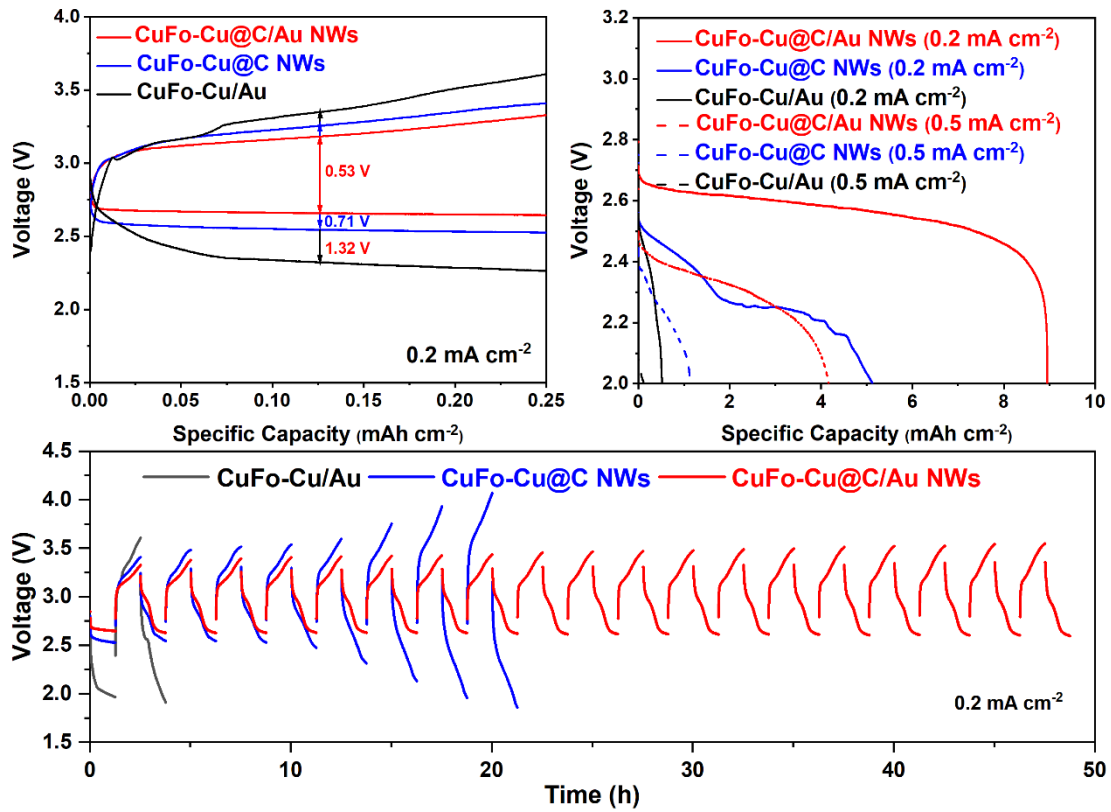
Figure S10. (a) initial discharge-charge profiles at 0.2 mA cm^{-2} with a limited capacity of 0.25 mAh cm^{-2}, (b) full discharge curve at two different current densities of 0.2 and 0.5 mA cm^{-2} with a cut-off voltage of 2 V, (c) cycling discharged/charged profiles at 0.2 mA cm^{-2} with 0.25 mAh cm^{-2}.
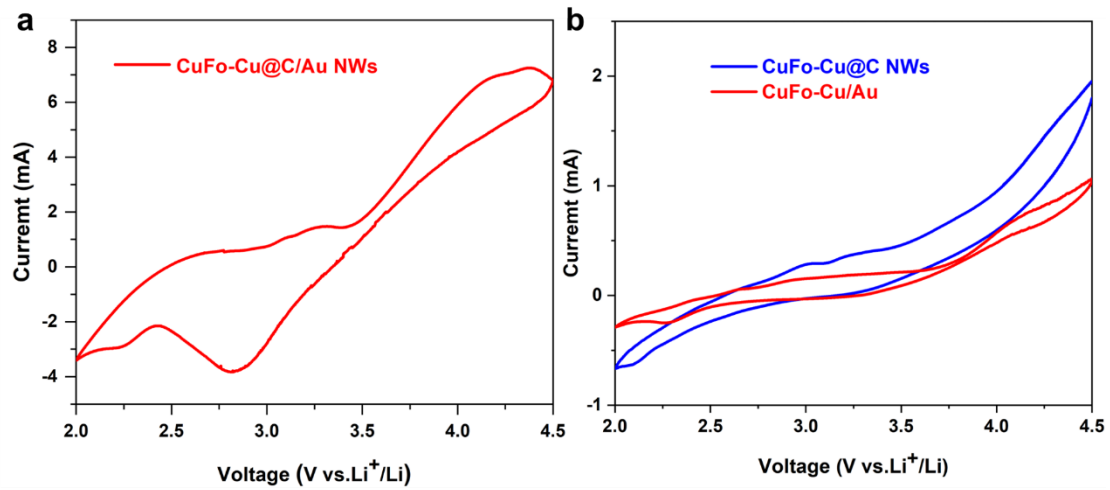
Figure S11. (a) CV curve of CuFo-Cu@C/Au NWs cathode at a sweeping rate of 1 mV s^{-1}, (b) CV curves of CuFo-Cu@C NWs and CuFo-Cu/Au cathodes at a sweeping rate of 1 mV s^{-1}.
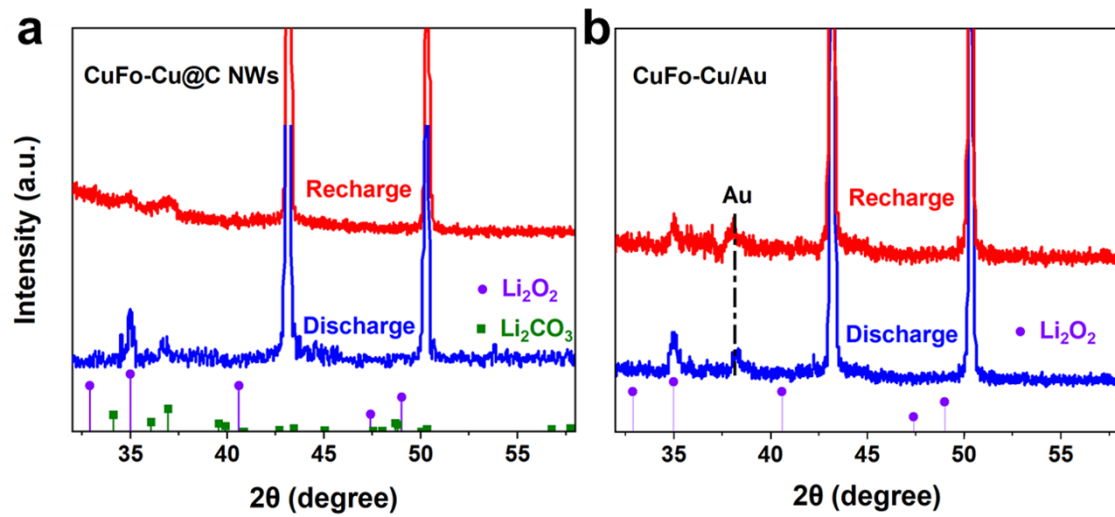
Figure S12. (a) XRD patterns of full discharge/recharge of CuFo-Cu@C NWs cathode; (b) XRD patterns of full discharge/recharge of CuFo-Cu/Au cathode.
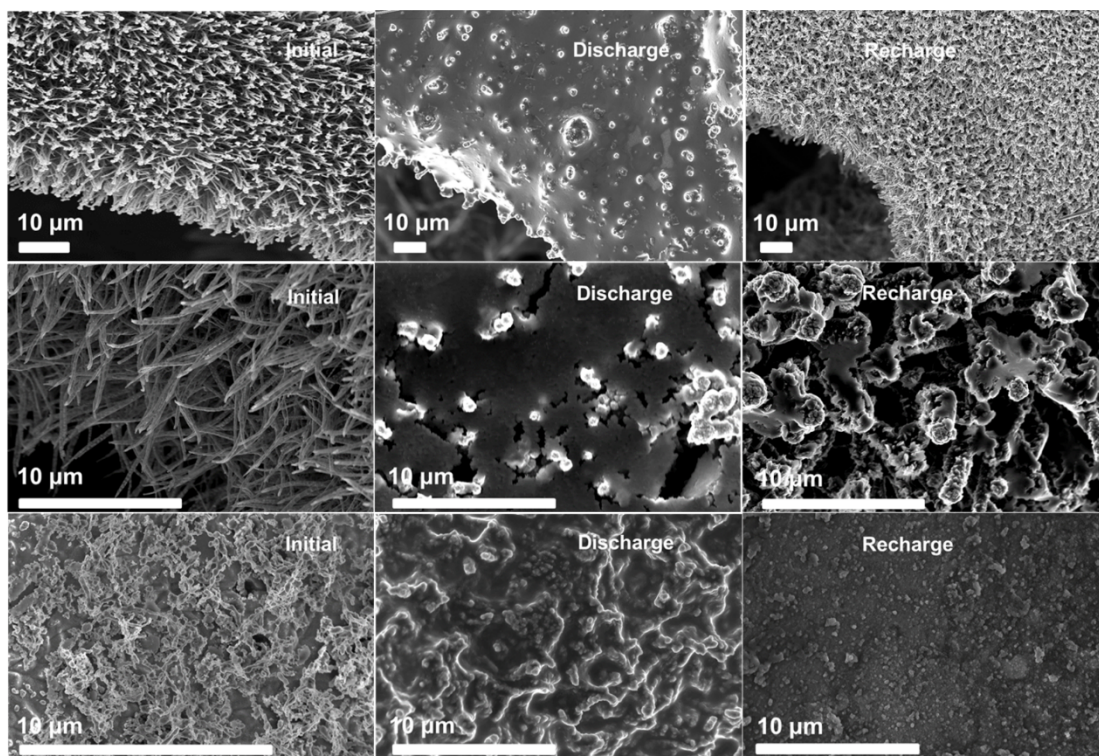
Figure S13. (a) to (c) SEM images of initial state, full discharge and recharge of CuFo-Cu@C/Au NWs, respectively; (d) to (f) SEM images of initial state, full discharge and recharge of CuFo-Cu@C NWs, respectively; (g) to (i) SEM images of initial state, full discharge and recharge of CuFo-Cu/Au NWs, respectively.
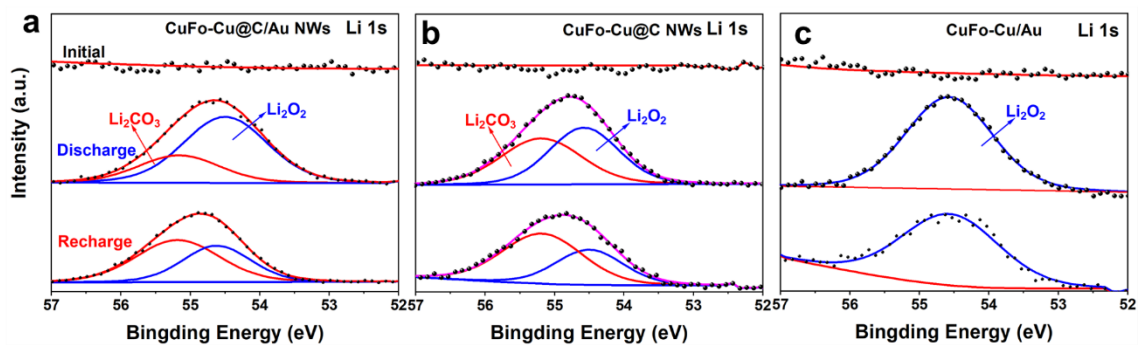
Figure S14. (a) to (c) XPS spectra of Li 1s for CuFo-Cu@C/Au NWs, CuFo-Cu@C NWs and CuFo-Cu/Au cathodes of initial state, full discharge-charge at 0.1 mA cm^{-2} with a cut-off discharge potential below 2 V and recharge potential over 4.5 V, respectively.
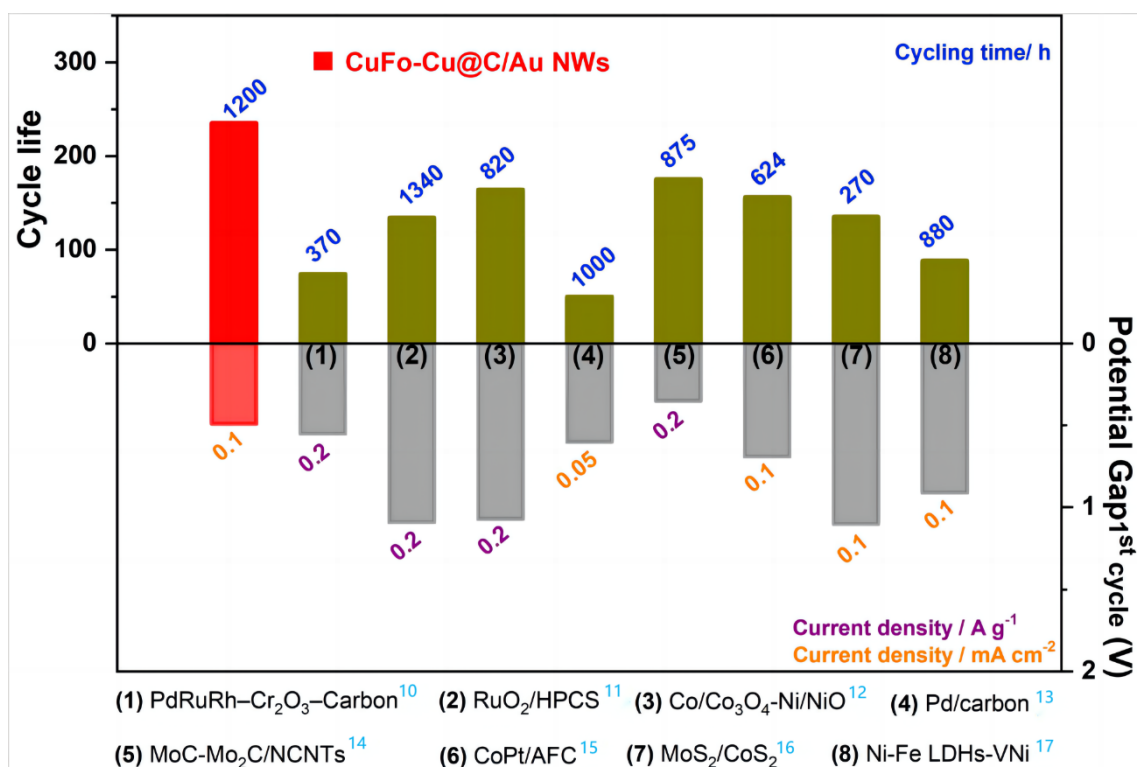
Figure S15. Superior cycling ability and small voltage gap under a high working current density in our work compared with previous reports.

References

1. G. Kresse and J. Hafner, *Physical Review B*, 1993, **47**, 558-561.

2. G. Kresse and J. Hafner, *Physical Review B*, 1994, **49**, 14251-14269.

3. G. Kresse and D. Joubert, *Physical Review B*, 1999, **59**, 1758-1775.

4. P. E. Blöchl, *Physical Review B*, 1994, **50**, 17953-17979.

5. Z. Wu, Y. Yu, G. Zhang, Y. Zhang, R. Guo, L. Li, Y. Zhao, Z. Wang, Y. Shen and G. Shao, *Adv. Sci.*, 2022, **9**, e2200614.

6. Y. Mo, S. P. Ong and G. Ceder, *Chem. Mater.*, 2012, **24**, 15-17.

7. Y. Yu, Z. Wang and G. Shao, *J. Mater. Chem. A*, 2019, **7**, 10483-10493.

8. H. Xu, G. Cao, Y. Shen, Y. Yu, J. Hu, Z. Wang and G. Shao, *Energy Environ. Mater.*, 2022, **5**, 852-864.

9. X. Cao, C. Wei, X. Zheng, K. Zeng, X. Chen, M. H. Rummeli, P. Strasser and R. Yang, *Energy Stor. Mater.*, 2022, **50**, 355-364.

10. T. Li, Q. Dong, Z. Huang, L. Wu, Y. Yao, J. Gao, X. Wang, H. Zhang, D. Wang, T. Li, R. Shahbazian-Yassar and L. Hu, *Adv. Mater.*, 2022, **34**, e2106436.

11. Z. Lian, Y. Lu, S. Zhao, Z. Li and Q. Liu, *Adv. Sci.*, 2023, **10**, e2205975.

12. L. Peng, J. Wang, S. Guo and C. Li, *Chem. Eng. J.*, 2022, **450**, 138252.

13.   T. Zhang, B. Zou, X. Bi, M. Li, J. Wen, F. Huo, K. Amine and J. Lu, *ACS Energy Lett.*, 2019, **4**, 2782-2786.

14.   Y. J. Oh, J. H. Kim, J. Y. Lee, S.-K. Park and Y. C. Kang, *Chem. Eng. J.*, 2020, **384**, 123344.

15.   H. Xia, Q. Xie, Y. Tian, Q. Chen, M. Wen, J. Zhang, Y. Wang, Y. Tang and S. Zhang, *Nano Energy*, 2021, **84**, 105877.

16.   D. Li, L. Zhao, Q. Xia, L. Liu, W. Fang, Y. Liu, Z. Zhou, Y. Long, X. Han, Y. Zhang, J. Wang, Y. Wu and H. Liu, *Small*, 2022, **18**, e2105752.

17.   Y. Zhou, D. Yan, Q. Gu, S. Zhu, L. Wang, H. Peng and Y. Zhao, *Appl. Catal. B,* 2021, **285,** 119792.